CHALMERS
UNIVERSITY OF TECHNOLOGY

In situ characterisation for studying nucleation and growth of nanostructured materials and thin films during liquid-based synthesis

Journal of Sol-Gel Science and Technology
https://doi.org/10.1007/s10971-022-05974-y

ORIGINAL PAPER: NANO-STRUCTURED MATERIALS (PARTICLES, FIBERS, COLLOIDS, COMPOSITES, ETC.)

In situ characterisation for studying nucleation and growth of nanostructured materials and thin films during liquid-based synthesis

Kristine Bakken [1,2] · Ola Gjønnes Grendal [1,3] · Mari-Ann Einarsrud [1]

Received: 15 September 2022 / Accepted: 19 October 2022

Abstract

Knowledge about the nucleation, growth, and formation mechanisms during materials synthesis using sol-gel and solution-based methods is important to design a material with desired properties. We used aqueous chemical synthesis as an environmentally friendly and highly flexible route to tailored and reproducible synthesis of oxide nanomaterials and thin films. For studies of hydrothermal synthesis an in situ cell using synchrotron X-ray diffraction was used to investigate the formation mechanisms of $Sr_xBa_{1-x}Nb_2O_6$ piezoelectrics. Aqueous chemical solution deposition of phase pure oriented piezoelectric thin films demands strong control of processing parameters. An in situ cell for synchrotron X-ray diffraction studies of the annealing and crystallisation steps during aqueous chemical solution deposition was used to understand the nucleation and crystallisation of $Ba_{0.85}Ca_{0.15}Zr_{0.1}Ti_{0.9}O_3$ (BCZT). We discuss how the knowledge about nucleation and growth obtained by in situ characterisation can be used to design the optimal procedure for fabrication of oxide materials with desired properties.

Graphical abstract

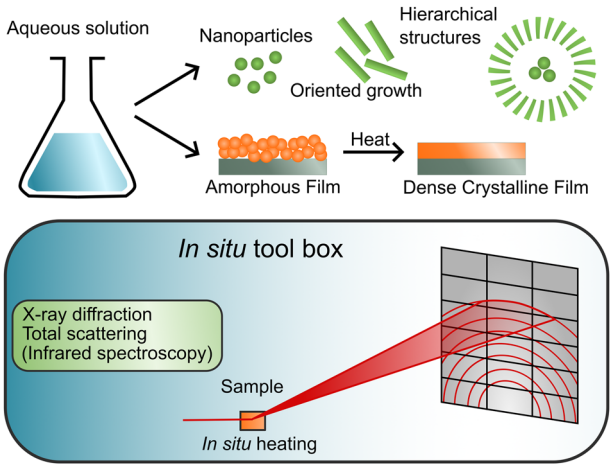

✉ Mari-Ann Einarsrud
mari-ann.einarsrud@ntnu.no

[1] Department of Materials Science and Engineering, NTNU Norwegian University of Science and Technology, Trondheim, Norway

[2] Present address: Department of Physics, Chalmers University of Technology, Gothenburg, Sweden

[3] Present address: European Synchrotron Radiation Facility (ESRF), 71 avenue des Martyrs, 38000 Grenoble, France

Published online: 09 November 2022

Keywords Oxide piezoelectrics · In situ characterisation · Hydrothermal synthesis · Thin film deposition · $Ba_{0.85}Ca_{0.15}Zr_{0.1}Ti_{0.9}O_3$ (BCZT) · $Sr_xBa_{1-x}Nb_2O_6$ (SBN)

Highlights

- In situ studies provide valuable insight allowing for simple ways to optimise synthesis parameters.
- A discussion about general guidelines for the aqueous synthesis of oxide materials is provided.
- Pre-nucleation clusters have proven important to tailor the formation and growth of the materials.
- Control of hydrothermal synthesis demands understanding of the chemistry.
- Film quality depends on chemistry of the precursor solution, intermediates, and the initial heating.

1 Introduction

Control of size, structure, and microstructure during the synthesis of nanomaterials and thin films is important to tailor materials properties. This is often a challenge using sol-gel and wet chemical synthesis methods as several parameters, e.g., type of precursors, concentration, type of solvent are determining the materials properties. To design materials, in situ characterisation techniques are a prerequisite to determine and control the reactions, nucleation, and growth mechanisms during the whole path of the synthesis. Synthesis from aqueous solutions is especially beneficial with respect to the environment and is being developed for several oxide systems including ferro- and piezoelectric materials.

In situ experiments during hydrothermal synthesis have been conducted for over 30 years since the early work by Polak et al. in 1990 [1], investigating the formation and growth of a wide range of materials. Since then, notable work has been done mostly on a range of binary oxides, using conventional powder diffraction techniques [2–4], total scattering [4–6] and small angle scattering [2, 7]. In later years, work on more complex oxides has been reported [8–10], with a special focus on perovskites [11–13]. In all these papers valuable system-specific insight has been gained. For example, Walton et al. [11] showed that $BaTiO_3$ formed through a dissolution-precipitation mechanism, as opposed to the topotactic transformation suggested based in ex situ kinetic studies [14]. Dalod et al. [15] used in situ characterisation to confirm an oriented attachment growth mechanism producing rod-shaped TiO_2 nanoparticles. Similarly, the formation of hopper-shaped particles could be rationalised based on insight about the pre-nucleation clusters and in situ data in the case of $Sr_xBa_{1-x}Nb_2O_6$ [16]. Pre-nucleation clusters have proven important to understand the formation and growth of several materials, for example for WO_3, where different pre-nucleation clusters were stable in different solvents, and found to directly influence the final atomic structure [6].

Chemical solution deposition (CSD) is a well-suited, inexpensive, and flexible method for fabrication of oxide thin films [17, 18]. Lead-containing ferroelectric films based on $Pb(Zr,Ti)O_3$ (PZT) are industrially produced by CSD, but synthesis routes for other ferroelectric materials have also been developed [2, 6]. The properties and microstructure of the thin films are reported to be heavily influenced by the synthesis parameters and procedure. Dependent on the temperature program used for annealing, decomposition, pyrolysis, and crystallisation reactions are taking place. The decomposition processes of the precursors during the deposition are typically not reported [19]. Hence, to produce high quality thin films from CSD, a thorough understanding of the complex decomposition and crystallisation reactions is desired to optimise the film processing conditions.

In situ growth of thin films investigated by synchrotron X-ray diffraction (XRD) are reported for PLD [20], magnetron sputtering [21] and thermal co-evaporation [22], all in a reflection geometry. In situ post-deposition annealing of oxide films grown by molecular-beam-epitaxy (MBE) [23] and in situ characterisation of the piezoelectric response from crystalline PZT films from CSD [24] have also been investigated. Total-scattering XRD of crystalline thin films on amorphous substrates have been reported in transmission [25] and reflection [26] geometry. A setup for in situ annealing of PZT thin films on Pt/Si substrates from CSD has been described, where infrared (IR) lamps were used, mimicking film annealing in rapid thermal processing (RTP) units [27, 28]. In our previous work, we designed a setup for in situ synchrotron XRD measurements on oxide thin films from aqueous CSD with a heating plate capable of heating rates up to 20 °C/s and temperatures of 1000 °C, mimicking the annealing in a conventional RTP unit [29]. $BaTiO_3$-based [30–32], $K_{0.5}Na_{0.5}NbO_3$ [33] and $Sr_{1-x}Ba_xNb_2O_6$ [34] thin films were monitored during crystallisation and texture formation was studied. Combined with in situ IR spectroscopy and in situ total scattering experiments on powders from the same precursor solutions the whole annealing process could be analysed and generalised mechanisms for tailoring thin films from CSD were developed.

Here, we present the application of in situ characterisation for studies of nucleation, growth, and orientation of nanostructured piezoelectric oxide materials by showing selected examples of the synthesis of lead-free piezoelectric

Table 1 Overview of the experiment names, temperature, pressure, Nb concentration and Sr + Ba concentration for the in situ X-ray diffraction experiments for the hydrothermal synthesis of SBN

Name	Temperature [°C]	Pressure [bar]	Nb concentration [M]	Sr + Ba concentration [M]
SBN50	300	200	0.25	0.13
SBN50_1/2 Nb	300	200	0.13	0.13

$Sr_{1-x}Ba_xNb_2O_6$ by hydrothermal synthesis and $Ba_{0.85}Ca_{0.15}Zr_{0.1}Ti_{0.9}O_3$ (BCZT) film deposition. A discussion about general guidelines for the aqueous synthesis of oxide nanostructures and thin films is provided based on our in situ characterisation research and relevant literature.

2 Experimental section

2.1 Hydrothermal synthesis and characterisation

Nominal composition $Sr_xBa_{1-x}Nb_2O_6$ (SBN, general formula $A1_{5x}A2_{5-5x}B1_2B2_8O_{30}$, with space group *P4bm* at room temperature) with $x = 0.5$ (SBN50) was prepared by mixing stochiometric amounts of strontium nitrate and barium nitrate with a niobic acid aqueous dispersion. The niobic acid was prepared by precipitation from an ammonium niobate (V) oxalate hydrate solution. More details about the synthesis were described previously [35]. The final precursor solution had a Nb-concentation of about 0.25 M. Additionally, a precursor solution with 0.13 M (SBN_1/2 Nb) Nb-concentration was prepared. Details for the two experiments performed are presented in Table 1.

The in situ XRD experiments were performed at the Swiss-Norwegian Beamlines (SNBL, BM01), European Synchrotron Radiation Facility (ESRF), Grenoble, France. The experimental setup consisted of a single crystal sapphire capillary pressured (200 bar) with a high-pressure liquid chromatography pump and heated with a high temperature heat blower (300 °C). The details about the experimental setup are described elsewhere [13, 36]. Data were collected in transmission mode using the *PILATUS@SNBL* platform, and 2D images were treated (masked for parasitic regions and integrated into 1D diffractograms) using *BUBBLE* [37]. The wavelength ($\lambda = 0.77445$ Å) was calibrated using LaB_6 (NIST 660a standard).

2.2 Thin film deposition and characterisation

$Ba_{0.85}Ca_{0.15}Zr_{0.1}Ti_{0.9}O_3$ (BCZT) thin films were prepared from a 0.23 M aqueous precursor solution by mixing separate Ba-, Ca-, Zr- and Ti-complex solutions in the desired stoichiometry. $Ba(NO_3)_2$ and $Ca(NO_3)_2 \cdot 4H_2O$ were stabilised in water with both citric acid and EDTA, while $ZrO(NO_3)_2 \cdot 6H_2O$ and Ti-isopropoxide were only stabilised with citric acid. Ammonia solution was used prior to mixing to adjust the solutions to a neutral pH. More details about the exact procedures have been reported previously [32, 38]. Single crystal (100) $SrTiO_3$ substrates were cleaned with oxygen plasma for 2 min to enhance wetting. The precursor solution was deposited onto the substrate through a syringe with a 0.2 mm filter and spin coated at 3500 rpm for 30 s. A single layer were deposited and dried on a hotplate for 4 min at 180 °C.

The in situ synchrotron X-ray diffraction experiments were performed at the BM01 end station at SNBL at ESRF. The BCZT films were heated on a rapid heating plate (RHP) described by Blichfeld et al. [29], while recording the diffractograms on a Pilatus2M 2D-detector in grazing incidence geometry. The wavelengths were 0.77624 and 0.78449 Å. The films were annealed in air and cooled by switching off the heat source. The recorded 2D diffractograms were reduced to 1D by the BM01 software tools [37] and compensated for thermal expansion by using the substrate reflections as an internal reference. For texture evaluation azimuthal slicing of the data was done and refined using MAUD [39] (with the E-WIMV model). Pole figures were prepared from the refined texture in the MTEX [40] package for MATLAB. More detailed descriptions of the experimental setup and data processing can be found in our previous work [32, 38].

3 Results and discussion

3.1 Hydrothermal synthesis of $Sr_{1-x}Ba_xNb_2O_6$

In our previous work, we observed that for high Sr-fractions (0.5 or higher) SBN, a secondary phase formed during the hydrothermal synthesis of SBN [35]. This secondary phase was found to be a pyrochlore type structure, containing Nb, Sr and Ba with significantly higher Sr fractions than in the SBN phase. From the in situ experiments we observed that the secondary phase always formed after the SBN phase. Based on this, two follow-up experiments are presented here to attempt to supress the formation of the secondary phase at high Sr-fractions. Firstly, a direct reproduction of one of our previous experiments as a reference was performed (SBN50). Secondly, one experiment where the amount of Nb was halved keeping all other synthesis parameters the same was performed (SBN50_1/2NB), with the hypothesis that the secondary phase would not form if the formation of SBN depletes the system for Nb.

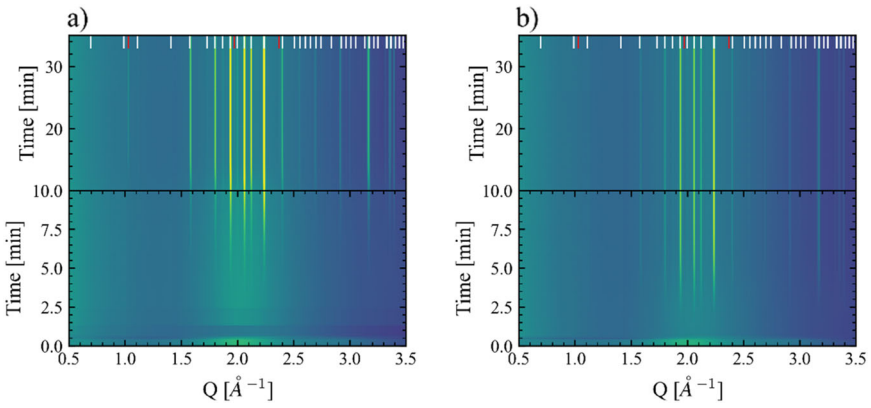

Fig. 1 XRD contour plot showing the formation of SBN from an amorphous precursor solution for (**a**) SBN50 and (**b**) SBN50_1/2 Nb. White ticks show expected reflections for SBN, while red ticks show characteristic reflections for the pyrochlore secondary phase. The pyrochlore phase only forms for SBN50

A contour plot showing the formation of SBN after ~3 min, and the pyrochlore secondary phase after ~10 min is presented in Fig. 1a for SBN50. This is in excellent agreement with our previous experiment with identical synthesis parameters [35], showing the great reproducibility of the synthesis route and the experimental setup. Figure 1b shows the contour plot for SBN50_1/2 Nb where only SBN forms. This result to a large degree confirms our hypothesis. These results will enable the hydrothermal synthesis of phase pure SBN even for high Sr-fractions and it shows the strength of performing in situ experiments for optimisation of synthesis parameters. As an additional note, the experiment where the concentration of Nb was doubled was also conducted, but this yielded only amorphous phase(s).

3.2 Aqueous film deposition of $Ba_{0.85}Ca_{0.15}Zr_{0.1}Ti_{0.9}O_3$

Previous work on $BaTiO_3$ thin films on various substrates [30] showed that for thin films annealed with a heating rate lower than 2 °C/s, textured samples were obtained by heating to temperatures above 700 °C. $BaTiO_3$ films heated with a heating rate of 0.2 °C/s displayed a high degree of preferred orientation determined by the substrate orientation. A similar experiment was performed on a BCZT thin film on (100) $SrTiO_3$ substrate. However, no degree of preferred orientation was detected in this sample after the heating procedure shown in Fig. 2. The diffractogram demonstrate that also BCZT displays the same type of intermediate phase observed for the $BaTiO_3$ [30, 31], seen by a weak diffraction line at 13.3°. The formation temperature for the intermediate phases and the nucleation temperature for BCZT is however, higher than for $BaTiO_3$, which is expected as the formation energy of $BaZrO_3$ is higher than for $BaTiO_3$ [41].

Since no texture was observed in the BCZT thin film after annealing with a heating rate of 0.2 °C/s, a second

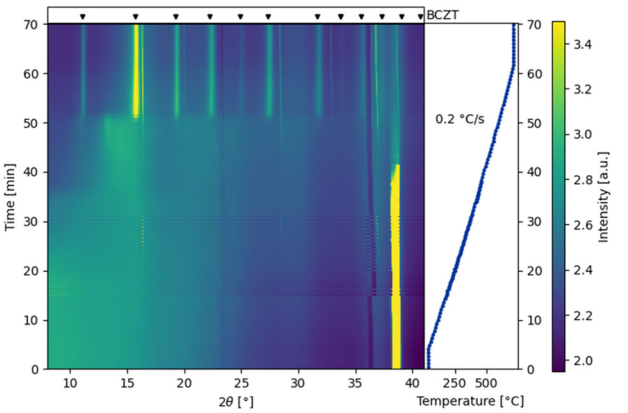

Fig. 2 XRD contour plot of a BCZT thin film on (100) STO as a function of time with the corresponding temperature profile. The intense peak at low temperatures at $2\theta = 38.6°$ is due to the unmasked (311) $SrTiO_3$ substrate reflection, where the loss of the peak intensity at higher temperatures was caused by the sample shifting slightly during the annealing. The apperent zig-zags in the diffractograms are a result to the data treatment to compensate for the thermal expansion [29]. The wavelength was 0.77624 Å

sample was heated to 800 °C with a heating rate of 0.03 °C/s, as heating rates in this range were observed to increase the degree of preferential orientation in $BaTiO_3$ thin films. Moreover, given the slower nucleation dynamics of BCZT compared to $BaTiO_3$, heating with a heating rate of 0.2 °C/s could be too fast for the BCZT system. This is indeed what was observed, as a heating rate of 0.03 °C/s resulted in a highly textured BCZT thin film. However, the contour plot is not included due to loss of beam during most of the annealing program. The room temperature diffractogram for the highly textured BCZT thin film is displayed in Fig. 3a, while the refined diffractogram from Rietveld refinements with a E-WIMV texture model is shown in Fig. 3b. Based on the texture refinement, pole figures were calculated, showing that the BCZT thin film follows the (100) orientation of the $SrTiO_3$ substrate (Fig. 3c).

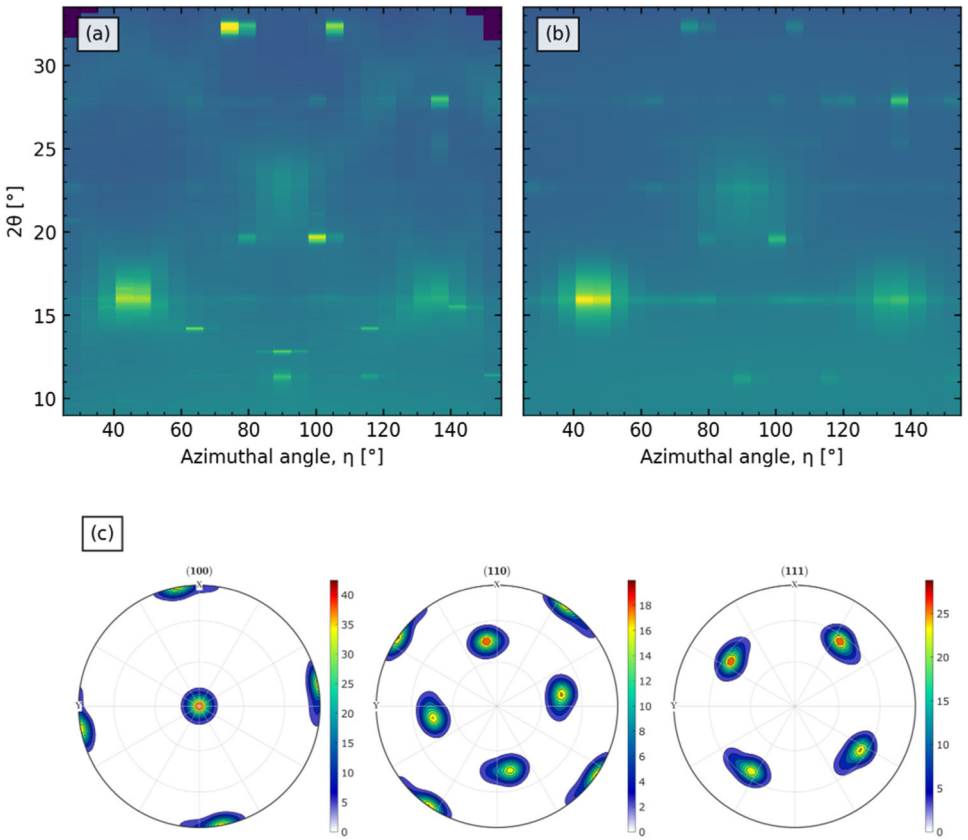

Fig. 3 Room temperature (**a**) experimental and (**b**) refined X-ray diffractograms and (**c**) pole figures from Rietveld refinements for a textured 20 nm (single layer) BCZT film on (100)$SrTiO_3$ substrate heated with a heating rate of 0.03 °C/s. The wavelength was 0.78449 Å

3.3 General guidelines for the aqueous synthesis of oxide nanostructures and thin films

3.3.1 Hydrothermal synthesis

Through the last 30 year of in situ experiments, system specific (i.e., for the specific materials and reaction conditions investigated) insight into the formation and growth has been obtained for a range of oxide materials. However, the high reaching goal for many of these studies has been to gain a fundamental understanding of the hydrothermal synthesis that is not necessarily system specific and provide generic theoretical models for nucleation and growth applicable to the synthesis of all materials. This will allow moving away from trial-and-error approaches when developing new synthesis routes, and potentially enable rational design of materials with controlled size, morphology, stoichiometry, and doping levels, which has been achieved for the synthesis of organic materials to some degree [42, 43]. So the question is: Have we achieved a fundamental understanding of the hydrothermal synthesis?

Trying to draw some general conclusions from existing literature on hydrothermal synthesis is a challenging task. Both because the focus of the different works is spread, but also because apparently similar materials with similar precursor chemistry show very different nucleation and growth mechanisms. For example, the hydrothermal synthesis of the three perovskites, $BaTiO_3$, $NaNbO_3$ and $KNbO_3$, proceeds very differently from their respective binary oxides (TiO_2 and Nb_2O_5) and dissolved metal hydroxides ($Ba(OH)_2$, NaOH and KOH) under alkaline conditions. $BaTiO_3$ forms via a dissolution-precipitation mechanism without any crystalline intermediates, with the complete reaction taking ~60 min at 200 °C [11]. A similar dissolution-precipitation mechanism was observed for $KNbO_3$, with the complete reaction taking ~35 min at 250 °C [12]. In contrast, the complete conversion of Nb_2O_5 into $NaNbO_3$ takes less than 5 min at 250 °C and proceeds through several crystalline intermediate phases [12]. The intermediates are later shown to directly influence the final size and morphology [13].

Another example is the synthesis of $Ce_xZr_{1-x}O_2$ ($x = 0.0$, 0.2, 0.5, 0.8, 1.0), where a distinct change in growth kinetics is reported as a function x, even though a continuous solid solution was obtained [3]. At high ceria content, the growth is initially limited by surface reaction kinetics and becoming limited by diffusion of monomers to the surface at larger particle sizes. For high zirconia content, the opposite is observed. Later, both the formation of CeO_2 ($x = 1$) and ZrO_2 ($x = 0$) have been investigated further with in situ X-ray total scattering, revealing significant differences in the pre- and early nucleation stages. In the case of

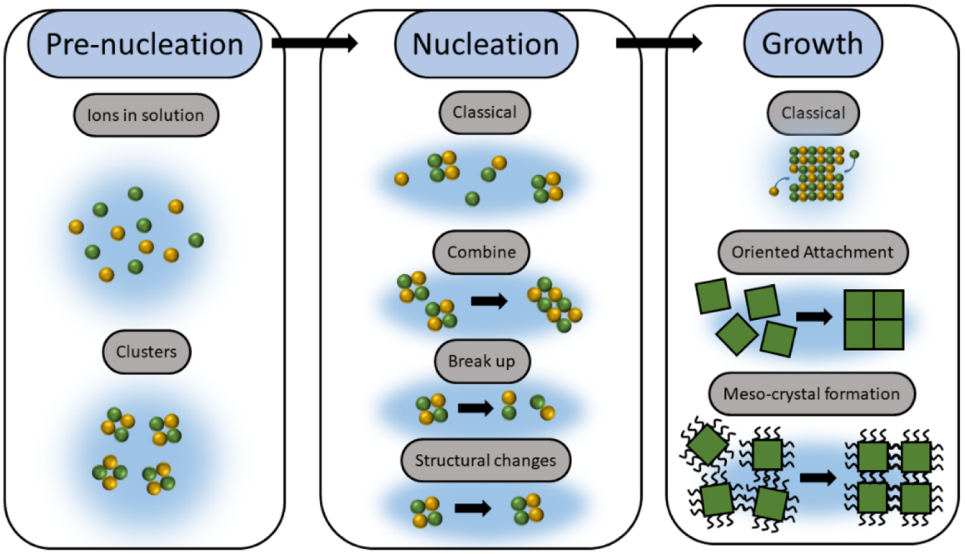

Fig. 4 Schematic illustration of possible nucleation and growth mechanisms during hydrothermal synthesis, showing both classical and non-classical mechanisms. This is not an exhaustive overview. For a real system, the reaction path is not necessarily a straight path from left to right

CeO_2, dimeric Ce(IV) nitrate pre-nucleation clusters are observed to assemble into CeO_2 [4], while for ZrO_2 chains of edge-sharing cyclic zirconium tetramers are observed to first break up into smaller clusters before assembly into ZrO_2 [5].

Furthermore, for the synthesis of WO_3 [6] and ZrO_2 [5], the effect of two different solvents were investigated giving different reaction routes and influencing the crystalline structure of the final product. In the case of WO_3, the α-Keggin polyoxotungstate was stable in the precursor solution in both water and oleylamine solvents. However, the reactions proceeded through different intermediate clusters in the two solvents, which in the end resulted in crystalline nanoparticles with a large degree of disorder and perfectly ordered in water and oleylamine, respectively [6]. The degree of disorder is rationalised based on the observed intermediate clusters and phases. A similar scheme is reported for ZrO_2, where the same cluster structure is stable in both water and methanol but undergoes different changes before crystallisation in the two solvents, which further controls the polymorph of the final crystalline ZrO_2 (monoclinic in water and mix of tetragonal and monoclinic in methanol) [5].

A schematic overview of possible nucleation and growth mechanisms are summarised in Fig. 4. Keeping in mind that this is not an exhaustive overview and that a reaction path for a given system is not necessarily a straight path from left to right, the complexity of the hydrothermal synthesis becomes apparent.

From the above discussion, it seems difficult to draw a general conclusion. For full control of the nucleation and growth during hydrothermal synthesis of inorganic materials, a fundamental understanding of the underlying chemistry of each system is necessary. The purely statistical models of classical nucleation and growth theory is in many cases too crude to capture the full picture, but not necessarily wrong, or useless, nonetheless. It seems unlikely that one single deterministic model for the nucleation and growth of all inorganic materials can be found. Instead, some predicting power can be sought for chemically similar systems by combining system specific chemical insight and generalised theories. For example, the work done on the niobium-based $NaNbO_3$, $KNbO_3$ and $K_xNa_{1-x}NbO_3$ [12, 13] have proven to give important insight for the development of the synthesis route for the niobium-based SBN [35] and the rationalisation of formation of SBN hopper-crystals [16]. One noteworthy observation is the impact in situ X-ray total scattering experiments have had on the field, enabling a view into the important pre- and early nucleation stages of the hydrothermal reaction. Finally, even if fully generic models cannot be achieved for the nucleation and growth during hydrothermal synthesis, in situ studies will provide valuable insight that can allow for simple ways of quickly optimise synthesis parameters, as highlighted in this work.

3.3.2 Chemical solution deposition

Nucleation and growth of films from CSD, are normally described using classical nucleation and growth theory, which is predicting the crystallisation process [17, 18], especially for materials systems where the typical organic solvents, such as 2-methoxyethanol, are used. An example is the typical columnar microstructure of PZT films from CSD resulting from heterogenous nucleation at the interface. However, there are many essential differences between different material systems, for example the columnar PZT versus polycrystalline $BaTiO_3$ (or $(Ba,Sr)TiO_3$), even though they share the same structure and related cations [17]. The discrepancy between the classical description and the material system specific decomposition, nucleation and

growth become even more evident considering thin films from aqueous CSD.

Our previous work on $BaTiO_3$-based thin films from aqueous CSD showed that nucleation of the perovskite occurred both through direct nucleation and through a topotaxial transformation from the intermediate nanosized calcite-like $BaCO_3$ and $BaTi_4O_9$ phases [30–32, 38]. It was shown that the processing conditions during formation and decomposition of the intermediates were just as important as those for the nucleation of the perovskite phase. Most notably, the texture formation in the perovskite phase was dependent on the total annealing time below the nucleation limit (and a suitable substrate) [30]. Moreover, it was demonstrated that unfavourable homogenous nucleation could be suppressed by rapid heating in the temperature window between nucleation of the perovskite and a threshold for where cube-on-cube growth is favourable at the substrate interface, resulting in relaxed epitaxial films [31]. In the case of $K_{0.5}Na_{0.5}NbO_3$ (KNN) from aqueous solutions, the change of complexing agent for the stabilisation of Nb increases the nucleation temperature drastically when oxalic acid is replaced my malic acid [33, 44], demonstrating the importance of the chemistry of the precursor solution. For both complexing agents, nucleation occurs by rearrangements of Nb-O-octahedra and the incorporation of alkali metals in-between the octahedra, with relatively small changes to the local structure before nucleation.

These examples highlight the contrast between what was observed and what classical nucleation theory predicts. Chemistry and kinetics matter just as much as thermodynamics when it comes to understanding the mechanisms governing thin film deposition from CSD. Armed with that information, one could imagine that the annealing reactions could be divided into two regions (Fig. 5). The reactions occurring at low temperatures are decided by the precursor chemistry, as the choice of solvent and cation-precursors, complexing agents and additives will govern which type of cation-complexes that form and which type of gelling behaviour the film will display. The nature of the cross-linking of the complexes in the solution forming during spinning and the lowest temperatures are important for how the whole decomposition and organic removal process occur. Traditional sol-gel processes based on organic solvents will form different gels than films made by aqueous-based solutions.

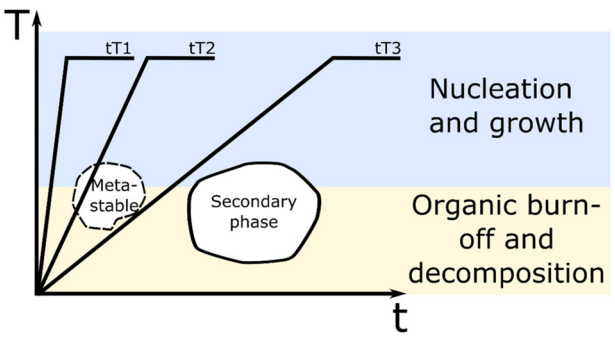

Fig. 5 time-Temperature diagram for oxide thin films from CSD illustrating that different decompostion and organic removal reactions occur at low temperatures while nucleation and growth depends on the intermdiate and themodynamically stable and metastable phases forming during the low temperature stage. Different heating profiles (tT1, tT2, and tT3) are expected to result in different film properties dependent on the the nature of the intermdiate phases, meaning that the heating profile should be tailored based on the precursor chemistry and desired properties of the final film

Given the chemistry of a specific precursor solution, there is a "landscape" in the time-Temperature (tT) diagram (Fig. 5) at low temperatures (yellow region) of possible intermediate and thermodynamically stable and metastable secondary phases that could form under certain processing conditions. Which phases that are present when crossing the temperature limit to nucleation (blue region) will then decide the condition for nucleation and growth in the thin film. The nucleation and growth process will again impact various aspects of the final film, such as microstructure, crystallographic texture, phase purity and physical and chemical properties. Therefore, even for the same precursor solution the different time-Temperature profiles (tT1, tT2, and tT3) in Fig. 5 would yield different qualities of the films. If a precursor solution that decomposed without formation of detrimental secondary phases (like PZT from organic solutions) was heated with tT1, it typically would result in a film with columnar microstructure as heterogenous interlayer nucleation occurs, as classical nucleation events occur. In contrast, the same temperature program for aqueous $BaTiO_3$-based films would result in a completely polycrystalline film, due to the non-classical nucleation process. For the synthesis of aqueous $BaTiO_3$-based films, like BCZT, a heating procedure like tT3 can be expected to result in highly textured films (Fig. 3), provided a suitable substrate is used. The resulting film from choosing a heating profile like tT2 would depend on the nature of the metastable phase because, although it is thermodynamically metastable, it could be kinetically stabilised, otherwise it could lead to cation segregating and therefore alter the nucleation and growth.

How to make high quality thin films by CSD, therefore, depends on the chemistry of the precursor solution and the nature of the cation-complexes forming in the solution and during the initial heating. Knowledge about which secondary phases might form in a certain system and how thermodynamically stable they are is of course important. In general, traditional sol-gel processes tend to follow classical nucleation and growth theory more often than aqueous-based precursor solutions, but there are of course exceptions. An educated guess could also be made by considering

similar materials systems, e.g., $BaTiO_3$ and $SrTiO_3$ seem to form the same type of carbonate intermediate phases and therefore a good starting point would be to use the same heating program for both, but the different thermodynamic stability of Ba-carbonate and Sr-carbonate should also be considered. In situ characterisation could here be used to reduce the amount of trial and failure in optimising the annealing of a new material system, especially with an initial guess based on existing literature on similar systems. As microstructure, texture, phase purity, strain and crystallinity are all governed by the annealing procedure, but also determining the quality and properties of the final film, care should be taken to tailor the annealing program taking all these aspects into consideration.

A final note in this discussion, the atmosphere during the annealing procedure was not discussed, but for fabricating metal oxide thin films from CSD, it is beneficial to have a certain oxygen partial pressure in the atmosphere. However, for some material systems, like $Bi_{0.5}Na_{0.5}TiO_3$ [45], using pure oxygen can improve phase purity and crystallinity.

4 Conclusion

In situ studies of nanostructured oxide materials and thin films provide valuable insight into nucleation, growth, and orientation, simplifying the optimisation of synthesis parameters. This insight is exemplified here for two lead-free piezoelectric systems; first showing the importance of the solution concentrations for the synthesis of phase pure SBN crystals by hydrothermal synthesis and secondly, illustrating the importance of the heating program for the deposition of textured BCZT films. A discussion about guidelines for the aqueous synthesis of these oxide nanostructures and thin films is provided, demonstrating the challenge in giving general guidelines for all systems. Despite this, the in situ characterisation studies provide a valuable predicting capability for understanding the chemistry during hydrothermal synthesis and show that the early/pre-nucleation stage have proven important to tailor the formation and growth of the materials. Moreover, thin film quality depends on chemistry of the precursor solution, intermediates, and the initial heating as well as the crystallisation conditions. In situ characterisation can therefore be used to reduce the amount of trial and failure in optimising the annealing of a new material system, especially with an initial guess based on existing literature on similar systems. Finally, it is worth noting that the literature now has become extensive enough, especially for some material systems, that we can start to harvest benefits when designing new synthesis routes.

Acknowledgements The Research Council of Norway is acknowledged for the support to the Norwegian Micro- and Nano-Fabrication Facility, NorFab, (245963/F50). Finally, we acknowledge the SNX council for allocation of the beamtimes at the Swiss-Norwegian Beamline (SNBL) synchrotron facilities at the ESRF (The European Synchrotron Radiation Facility, Grenoble, France) and the SNBL beamline staff (Dr Wouter van Beek and Dr Dmitry Chernyshov) for their support and discussions during the experiments. Dr Anders Bank Blichfeld and Dr Kenneth Marshall are acknowledged for scientific input, discussions and help at the beamtime.

Author contributions All authors contributed to the study conception and design. Material preparation, data collection and analysis were performed by Kristine Bakken and Ola Gjønnes Grendal. The first draft of the manuscript was written by all authors and all authors commented on previous versions of the manuscript. All authors read and approved the final manuscript.

Funding This work was supported by NTNU and The Research Council of Norway under the Toppforsk program to the project (250403) "From Aqueous Solutions to oxide Thin films and hierarchical Structures" (FASTS). Open access funding provided by NTNU Norwegian University of Science and Technology (incl St. Olavs Hospital - Trondheim University Hospital).

Compliance with ethical standards

Conflict of interest The authors declare no competing interests.

References

1. Polak E, Munn J, Barnes P, Tarling SE, Ritter C (1990) Time-resolved neutron diffraction analyses of hydrothermal syntheses using a novel autoclave cell. J Appl Cryst. https://doi.org/10.1107/S0021889890002473
2. Bremholm M, Felicissimo M, Iversen BB (2009) Time-resolved in situ synchrotron X-ray study and large-scale production of magnetite nanoparticles in supercritical water. Angew Chemie Int Ed. https://doi.org/10.1002/anie.200901048
3. Tyrsted C, Becker J, Hald P, Bremholm M, Pedersen JS, Chevallier J, Cerenius Y, Iversen SB, Iversen BB (2010) In-situ synchrotron radiation study of formation and growth of crystalline $Ce_xZr_{1-x}O_2$ nanoparticles synthesized in supercritical water. Chem Mater. https://doi.org/10.1021/cm903316s
4. Tyrsted C, Jensen KMO, Bøjesen ED, Lock N, Christensen M, Billinge SJL, Iversen BB. (2012) Understanding the formation and evolution of ceria nanoparticles under hydrothermal conditions. Angew Chemie. https://doi.org/10.1002/ange.201204747

5. Dippel AC, Jensen KMO, Tyrsted C, Bremholm M, Bojesen ED, Saha D, Birgisson S, Christensen M, Billinge SJL, Iversen BB. (2016) Towards atomistic understanding of polymorphism in the solvothermal synthesis of ZrO_2 nanoparticles. Acta Crystallography A. https://doi.org/10.1107/S2053273316012675
6. Juelsholt M, Lindahl Christiansen T, Jensen KMØ. (2019) Mechanisms for tungsten oxide nanoparticle formation in solvothermal synthesis: from polyoxometalates to crystalline materials. J Phys Chem C. https://doi.org/10.1021/acs.jpcc.8b12395
7. Hinterberger S, Tscheließnig R, Jungbauer A. (2018) Anisotropic assembly during heat-up: the early stage hydrothermal synthesis of TiO_2 from a complexed precursor. ChemNanoMat. https://doi.org/10.1002/cnma.201800326
8. Chen J, Bai J, Chen H, Graetz J. (2011) In situ hydrothermal synthesis of $LiFePO_4$ studied by synchrotron X-ray diffraction. J Phys Chem Letters. https://doi.org/10.1021/jz2008209
9. Birgisson S, Jensen KMO, Christiansen TL, von Bulow JF, Iversen BB. (2014) In situ powder X-ray diffraction study of the hydro-thermal formation of $LiMn_2O_4$ nanocrystallites. Dalton Trans. https://doi.org/10.1039/C4DT01307G
10. Bøjesen ED, Jensen KMØ, Tyrsted C, Mamakhel A, Andersen HL, Reardon H, Chevalier J, Dippel AC, Iversen BB. (2026) The chemistry of $ZnWO_4$ nanoparticle formation. Chem Sci. https://doi.org/10.1039/C6SC01580H
11. Walton RI, Millange F, Smith RI, Hansen TC, O'Hare D. (2001) Real time observation of the hydrothermal crystallisation of barium titanate using in situ neutron powder diffraction. J Am Chem Soc. https://doi.org/10.1021/ja011805p
12. Skjærvø SL, Sommer S, Nørby P, Bøjesen ED, Grande T, Iversen BB, Einarsrud MA. (2017) Formation mechanism and growth of $MNbO_3$, M=K, Na by in situ X-ray diffraction. J Am Chem Soc. https://doi.org/10.1111/jace.14932
13. Skjærvø SL, Wells KH, van Beek W, Grande T, Einarsrud MA. (2018) Kinetics during hydrothermal synthesis of nanosized $K_xNa_{1-x}NbO_3$. CrystEngComm. https://doi.org/10.1039/C8CE01178H
14. Hertl W. (1988) Kinetics of barium titanate synthesis. J Am Chem Soc. https://doi.org/10.1111/j.1151-2916.1988.tb07540.x
15. Dalod ARM, Grendal OG, Skjærvø SL, Inzani K, Selbach SM, Henriksen L, van Beek W, Grande T, Einarsrud MA. (2017) Controlling oriented attachment and in situ functionalisation of TiO_2 nanoparticles during hydrothermal synthesis with APTES. J Phys Chem C. https://doi.org/10.1021/acs.jpcc.7b02604
16. Grendal OG, Nylund IE, Blichfeld AB, Tominaka S, Ohara K, Selbach SM, Grande T, Einarsrud MA (2020) Controlled growth of $Sr_xBa_{1-x}Nb_2O_6$ hopper- and cube-shaped nanostructures by hydrothermal synthesis. Chem. Eur. J. https://doi.org/10.1002/chem.202000373
17. Schwartz RW, Schneller T, Waser R. (2004) Chemical solution deposition of electronic oxide films. Comptes Rendus Chimie. https://doi.org/10.1016/j.crci.2004.01.007
18. Bassiri-Gharb N, Bastani Y, Bernal A (2014) Chemical solution growth of ferroelectric oxide thin films and nanostructures. Chem Soc Rev. https://doi.org/10.1039/C3CS60250H
19. Acosta M, Novak N, Rojas V, Patel S, Vaish R, Koruza J, Rossetti GA, Rödel J (2017) $BaTiO_3$-based piezoelectrics: Fundamentals, current status, and perspectives. Appl Phys Rev. https://doi.org/10.1063/1.4990046
20. Bauer S, Rodrigues A, Baumbach T (2018) Real time in situ X-ray diffraction study of the crystalline structure modification of $Ba_{0.5}Sr_{0.5}TiO_3$ during post-annealing. Sci Rep. https://doi.org/10.1038/s41598-018-30392-y
21. Roelsgaard M, Dippel AC, Andersen Borup K, Nielsen IG, Nyborg Broge N, Röh JT, Gutowski O, Iversen BB (2019) Time-resolved grazing-incidence pair distribution functional during deposition by radio-frequency magnetron sputtering. IUCrJ. https://doi.org/10.1107/S2052252519001192
22. Kaune G, Hartnauer S, Scheer R (2014) In situ XRD investigation of $Cu_2ZnSnSe_4$ thin film growth by co-evaporation. Phys Status Solidi. https://doi.org/10.1002/pssa.201330340
23. Bertram F, Deiter C, Pflaum K, Suendorf M, Otte C, Wollsshläger J (2011) In-situ X-ray diffraction studies on post-deposition vacuum-annealing of ultra-thin iron oxide films. J Appl Phys. https://doi.org/10.1063/1.3661655
24. Davydok A, Cornelius TW, Mocuta C, Lima EC, Araujo EB, Thomas O (2016) In situ X-ray diffraction studies on the piezoelectric response of PZT thin films. Thin Solid Films. https://doi.org/10.1016/j.tsf.2016.01.045
25. Jensen KMØ, Blichfeld BB, Bauers SR, Wood SR, Doooryhee E, Johnson DC, Iversen BB, Billinge SJ (2015) Demonstration of thin film pair distribution function analysis (tfPDF) for the study of local structure in amorphous and crystalline thin films. IUCrJ. https://doi.org/10.1107/S2052252515012221
26. Dippel AC, Roelsgaard M, Boettger U, Schneller T, Gutowski O, Ruett U (2019) Local atomic tructure of thin and ultrathinfils via rapid high-energy X-ray total scattering at grazing incidence. IUCrJ. https://doi.org/10.1107/S2052252519000514
27. Nittala K, Mhin S, Jones JL, Robinson DS, Ihlefeld JF, Brennecka GL (2012) In situ X-ray diffraction of solution-derived ferroelectric thin films for queantitiative phase and texture evolution mearurement. J Appl Phys. https://doi.org/10.1063/1.4766387
28. Nittala K, Mhin S, Dunnigan KM, Robinson DS, Ihlefeld JF, Kotula PG, Brennecka GL, Jones JL (2013) Phase and texture evolution in solution deposited lead zirconate titanate thin films: Formation and role of the Pt3Pb intermetallic phase. J Appl Phys. https://doi.org/10.1063/1.4811687
29. Blichfeld AB, Bakken K, Chernyshov D, Glaum J, Grande T, Einarsrud MA (2020) Experimental setup for high-temperature in situ studies of crystallisation of thin films with atmospheric control. J Synchrotron Rad. https://doi.org/10.1107/S1600577520010140
30. Bakken K, Blichfeld AB, Chernyshov D, Grande T, Glaum J, Einarsrud MA (2020) Mechanisms for texture in BaTiO3 thin films from aqueous chemical solution deposition. J Sol-Gel Sci Tech. https://doi.org/10.1007/s10971-020-05356-2
31. Bakken K, Pedersen VH, Blichfeld AB, Nylund IE, Tominaka S, Ohara K, Grande T, Einarsrud MA (2021) Structures and role of the intermediate phased on the crystallisation of $BaTiO_3$ from an aqueous synthesis route. ACS Omega. https://doi.org/10.1021/acsomega.1c00089
32. Bakken K, Blichfeld AB, Nylund IE, Chernyshov D, Glaum J, Grande T, Einarsrud MA (2021) Tailoring preferential orientation in $BaTiO_3$-based thin films from aqueous chemical solution deposition. Chemistry-Methods. https://doi.org/10.1002/cmtd.202100064
33. Bakken K, Gaukås NH, Grendal OG, Blichfeld AB, Tominaka S, Ohara K, Chernyshov D, Glaum J, Grande T, Einarsrud MA (2021) In situ X-ray diffraction studies of the crystallisation of $K_{0.5}Na_{0.5}NbO_3$ powders and thin films from an aqueous synthesis route. Open Ceramics. https://doi.org/10.1016/j.oceram.2021.100147
34. Pedersen VH, Blichfeld AB, Bakken K, Chernyshov D, Grande T, Einarsrud MA (2022) Crystallisation and texturing of $Sr_{1-x}Ba_xNb_2O_6$ thin films prepared by aqueous solution deposition – An in situ X-ray diffraction study. Cryst Growth Des. https://doi.org/10.1021/acs.cgd.2c00553
35. Grendal OG, Blichfeld AB, Vu TD, van Beek W, Selbach SM, Grande T, Einarsrud MA (2019) Composition and morphology tuning during hydrothermal synthesis of $Sr_xBa_{1-x}Nb_2O_6$ tetragonal tungsten bronzes studied by in situ X-ray diffraction. CrystEngComm. https://doi.org/10.1039/C9CE01049A

36. Becker J, Bremholm M, Tyrsted C, Pauw B, Jensen KMØ, Eltzholt J, Christensen M, Iversen BB (2010) Experimental setup for in situ X-ray SAXA/WAXS/PDF studies of the formation and growth of nanoparticles in near- and supercritical fluids. J. Appl. Crystallogr. https://doi.org/10.1107/S0021889810014688
37. Dyadkin V, Pattison P, Dmitriev V, Chernyshov D (2016) A new multipurpose diffractometer PILATUS@SNBL. J Synchrotron Radiat. https://doi.org/10.1107/S1600577516002411
38. Khomyakova E, Wenner S, Bakken K, Schultheiss J, Grande T, Glaum J, Einarsrud MA (2020) On the formation mechanism of $Ba_{0.85}Ca_{0.15}Zr_{0.1}Ti_{0.9}O_3$ thin films by aqueous chemical solution deposition. J Eur Cer Soc. https://doi.org/10.1016/j.jeurceramsoc.2020.07.042
39. Lutterotti L (2010) Total pattern fitting for the combined size-strain-stress-texture determination in thin film diffraction. Nucl Inst Meth Phys Res Section B: Beam Inter Mat Atoms. https://doi.org/10.1016/j.nimb.2009.09.053
40. Hielscher R, Schaaben H (2008) A novel pole figure inversion method: Specification of the MTEX algorithm. J Appl Cryst. https://doi.org/10.1107/S0021889808030112
41. Bera J, Rout SK (2005) On the formation mechanism of $BaTiO_3$-$BaZrO_3$ solid solution through solid-oxide reaction. Mat Lett. https://doi.org/10.1016/j.matlet.2004.07.053
42. El-Kaderi HM, Hunt JR, Mendoza-Cortés JL, Côté AP, Taylor RE, Keeffe M, Yaghi OM (2007) Designed synthesis of 3D covalent organic frameworks. Science. https://doi.org/10.1126/science.1139915
43. Bøjesen ED, Iversen BB (2016) The chemistry of nucleation. CrystEngComm. https://doi.org/10.1039/C6CE01489E
44. Gaukås NH, Dale SM, Ræder TM, Toresen A, Holmestad R, Glaum J, Einarsrud MA, Grande T (2019) Controlling phase purity and texture of $K_{0.5}Na_{0.5}NbO_3$ thin films by aqueous chemical solution deposition. Materials. https://doi.org/10.3390/ma12132042
45. Christensen M, Einarsrud MA, Grande T (2017) Fabrication of lead-free $Bi_{0.5}Na_{0.5}TiO_3$ thin films by aqueous chemical solution deposition. Materials. https://doi.org/10.3390/ma10020213